Chinese Chemical Letters 31 (2020) 2549–2555

Contents lists available at ScienceDirect

Chinese Chemical Letters

journal homepage: www.elsevier.com/locate/cclet

Review

Low-temperature selective catalytic reduction of NO_x with NH_3 over zeolite catalysts: A review

Yijuan Pu[a], Xinyu Xie[a], Wenju Jiang[a,b], Lin Yang[a,b], Xia Jiang[a,b], Lu Yao[a,b,*]

[a] College of Architecture and Environment, Sichuan University, Chengdu 610065, China
[b] National Engineering Research Center for Flue Gas Desulfurization, Sichuan University, Chengdu 610065, China

ARTICLE INFO

Article history:
Received 24 February 2020
Received in revised form 24 March 2020
Accepted 7 April 2020
Available online 17 April 2020

Keywords:
Selective catalytic reduction
NO_x
Zeolite
Catalyst
SO_2 and H_2O resistance

ABSTRACT

The selective catalytic reduction (SCR) of NO_x by NH_3 is one of the most mature technologies for NO_x treatment. Catalysts are the main factors affecting denitrification efficiency. Zeolites as low-temperature NH_3-SCR catalysts have been extensively studied in the past few years. In this work, the mechanism of zeolites for NH_3-SCR reaction was reviewed and the denitrification performances of zeolite catalysts prepared by different methods were compared. The effects of sulfur and water poisoning on zeolite catalysts in NH_3-SCR reaction were also analyzed. Several ways to address the problems in low-temperature NH_3-SCR reaction were discussed. Hopefully, this review could provide a fundamental understanding of SCR reaction on zeolite catalysts and pave the way toward similar studies to realize its commercial applications.

1. Introduction

Nitrogen oxides (NO_x) are the major source of air contamination [1,2]. Presently, nitrogen oxide control methods involve selective catalytic reduction of NO_x (SCR) [3,4], selective non-catalytic reduction, electron beam method, liquid absorption method [5], adsorption method [6], catalytic oxidation method, and catalytic decomposition method [7]. Among these methods, SCR is the most widely used technology because of its relatively high denitrification efficiency and low cost [8–10].

In the SCR process, the reductant preferentially reacts with NO_x on the catalyst in the presence of O_2, and toxic-free products N_2 and H_2O are released [11]. The key point of SCR technology is the catalyst [12,13]. The number and distribution of the active sites on the catalyst are affected by the catalyst support. The physical and chemical stability of the support also plays an important role in the performance of the active components of the catalyst. The active components of the SCR catalyst contain noble metals, and metal oxides [14]. The catalyst supports include pillared interlayer clays (PILC) [15], carbon-based materials [16,17], Al_2O_3 [18], CeO_2 [19], TiO_2 [20]and zeolites [21].

V_2O_5–$WO_3(MoO_3)/TiO_2$ was developed for industrial applications in 300−400 °C, but it showed poor catalytic activity at low temperature, and the toxicity of VO_x is also an inevitable disadvantage [22]. Thus, developing an economical and effective low temperature SCR catalyst is the key to low temperature denitrification.

Zeolites catalysts have been used for vehicles NH_3-SCR due to their high thermal stability, broad temperature windows and special active sites of isolated ion [23]. For low temperature flue gas SCR, zeolites are also the promising catalysts. Metal exchanged zeolites could regulate the electric field intensity, pore size and surface acidity of crystals, and zeolites could guide the local distribution of the main active components of catalysts [24,25].

In this paper, the NH_3-SCR reaction process of zeolite catalysts for denitrification at low temperature was reviewed. The mechanism of zeolites for SCR reaction was introduced in detail. The denitrification performance of different metal-modified zeolite catalysts was compared. In addition, sulfur and water poisoning on NH_3-SCR reaction over zeolite catalysts was summarized.

2. NH_3-SCR reaction

2.1. Process of low-temperature NH_3-SCR

The commercial V_2O_5–$WO_3(MoO_3)/TiO_2$ catalysts are not suitable for elimination NO_x from diesel vehicles, due to the narrow work temperature window and weak hydrothermal stability. Thus, zeolite catalysts have attracted attention for vehicles NH_3-SCR. For stationary sources, the NH_3-SCR reactor has three different arrangements, namely, high-dust, low-dust,

* Corresponding author at: College of Architecture and Environment, Sichuan University, Chengdu 610065, China.
E-mail address: yaolu@scu.edu.cn (L. Yao).

https://doi.org/10.1016/j.cclet.2020.04.012

and tail arrangements. Under the high-dust arrangement, the catalyst is more likely to be poisoned and blocked by fly ash. Under the low-dust arrangement, the SO_x in flue gas would poison the catalyst. For the tail arrangement, the NH_3-SCR reactor is placed behind the dust collector and desulfurization system so the catalyst is avoided by fly ash and SO_x poison. However, the temperature is relatively low (100–250 °C). Thus, a catalyst suitable for low-temperature SCR is required to avoid the re-heating of flue gas for denitrification.

2.2. Catalysts of NH_3-SCR reaction

The active components of catalyst contain noble metals [26], metal oxides [27], and vanadium-titanium catalysts [20,28]. Noble metal catalysts including P, Pd, Rh and Au, have been studied in the early stage of the NH_3-SCR reaction [25,29]. Noble metals are usually loaded on alumina, silicon oxide, and zirconia by iron exchanged with K, Na, and Ca to prepare catalysts. These catalysts were widely used in automobile exhaust purifiers in the 1970s. Despite the high catalytic activity at low temperature of noble metal catalysts, they are unsuitable for NO_x treatment of large-scale stationary sources due to their narrow active window and high cost [30]. Consequently, noble metal catalysts were gradually replaced by metal oxide catalysts and are only used in low-temperature catalysis and automobile exhaust gas treatment. Metal oxide catalysts have been widely used in SCR reaction [31], due to their advantages of low cost, good stability, and strong low-temperature activity and selectivity, and V_2O_5, MnO_x, Fe_2O_3, CuO, CeO_2 and their mixtures are usually used as the active components [32–34], and TiO_2 and Al_2O_3 are widely used as support to provide the catalyst a micropore structure and high specific surface area. Vanadium-titanium catalysts are widely used in the denitrification process of power plants [35,36]. The main vanadium catalysts supported by anatase TiO_2 are V_2O_5/TiO_2 [37], V_2O_5-WO_3/TiO_2 [38], V_2O_5-MoO_3/TiO_2 [39] and V_2O_5-WO_3-MoO_3/TiO_2 [40], which are used in industrial applications. Given its catalytic activity and resistance to SO_2 and H_2O, V_2O_5-WO_3/TiO_2 gradually replaced V_2O_5/TiO_2 [41].

The supports of the catalyst include zeolites, PILCs, carbon-based materials, and TiO_2. PILCs are prepared *via* the columnization process with the expansibility of some clay under the action of strong polar molecules and the exchange of cations [42]. Despite its high specific surface area and pores under different acidic conditions, the preparation of PILCs is complicated [43]. Carbon-based materials usually have developed pore structure, strong adsorption and good chemical stability [44]. Carbon-based materials contain active carbon (AC) [45], active carbon fiber (ACF) [46] and carbon nanotubes (CNTs) [47]. Due to its wide range of sources, low price and easy regeneration, AC is widely used. However, the NH_3-SCR reaction is an exothermic reaction that might lead to local heat accumulation on the catalysts during the NH_3-SCR process, which will destroy the pore structure of AC. ACF/CNTs have a better NH_3-SCR activity than AC, and ACF could even directly reduce NO_x to N_2. ACF/CNTs also have good mechanical strength and toughness that greatly reduce the wear rate in the application process [48]. However, the high price of ACF/CNTs limits the commercial application of ACF/CNTs catalysts. TiO_2, which is cheap and non-toxic, is the main support of metal oxide catalyst [49]. However, the catalyst supported by TiO_2 could not work efficiently at low temperature, and the active component (V_2O_5) is highly toxic, and shows high SO_2 oxidation [50].

Zeolites are a kind of aqueous compounds of crystalline aluminosilicate [51,52].Given their special pore structure and rich acidic sites, zeolite catalysts show good catalytic activity, high selectivity and wide active temperature window [53].

3. Mechanism of NH_3-SCR reaction on zeolites

NH_3-SCR technology selectively reduces NO_x to harmless N_2 and H_2O at a certain temperature (generally about 150–500 °C) over a catalyst. The mechanism of NH_3-SCR reaction is shown in Fig. 1.

The main reaction forms are as follows (Eqs. 1 and 2) [54,55]:

$$4NH_3 + 4NO + O_2 \rightarrow 4N_2 + 6H_2O \quad (1)$$

$$2NH_3 + NO + NO_2 \rightarrow 2N_2 + 3H_2O \quad (2)$$

Eq. 1 is the main reaction when the reaction temperature is lower than 400 °C, and the NO_x reacts with the injected NH_3 reductant at a stoichiometric ratio of 1:1 [56]. When the content of O_2 in the reaction system is too low, the following reactions might occur (Eq. 3):

$$4NH_3 + 6NO \rightarrow 5N_2 + 6H_2O \quad (3)$$

By contrary, an excessively high content of O_2 would lead to the occurrence of side reactions, which would not only reduce the NO conversion and N_2 selectivity, but also generate greenhouse gas N_2O, causing secondary pollution. The side reactions are as follows (Eqs. 4–9) [57,58].

$$3NO \rightarrow N_2O + NO_2 \quad (4)$$

$$4NH_3 + 3O_2 \rightarrow 2N_2 + 6H_2O \quad (5)$$

$$2NH_3 + 2O_2 \rightarrow N_2O + 3H_2O \quad (6)$$

$$4NH_3 + 4O_2 \rightarrow 4NO + 6H_2O \quad (7)$$

$$4NH_3 + 4NO + 3O_2 \rightarrow 4N_2O + 6H_2O \quad (8)$$

$$4NH_3 + 4NO_2 + O_2 \rightarrow 4N_2O + 6H_2O \quad (9)$$

The reactions in Eqs. 5–7 are the oxidation reactions of NH_3, which generally occur above 200 °C and intensify above 450 °C [59,60]. Thus, in the practical flue gas denitrification process, the reaction temperature is generally controlled below 450 °C. However, the side reaction formulas (Eqs. 8 and 9) still occur at a low temperature of 200 °C or even lower.

Xin *et al.* studied the NH_3-SCR reaction over Cu/SAPO-44. Their results showed that the SCR reaction on Cu-SAPO-44 follows a possible Eley-Rideal (E-R) mechanism, in which the coordinated NH_3 on Lewis acid sites preferentially reacts with the gaseous $NO + O_2$ at 150 °C [60]. Above 200 °C, the NH_3 from Brønsted acid

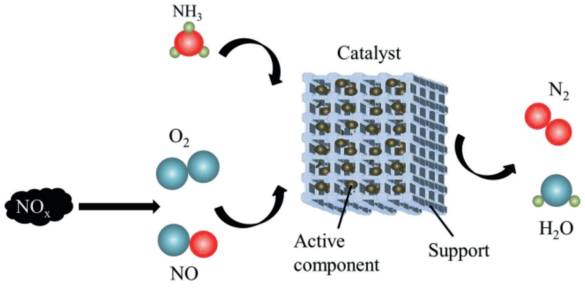

Fig. 1. Mechanism of NH_3-SCR reaction.

sites participated in the SCR reaction. Zhou *et al.* [61] reported two possible reaction paths over Fe-Ce-Mn/ZSM-5 catalyst for NH_3-SCR reaction. One is the bonding of NO_2 to the B acid center NH_4^+ to form $[NH_4^+]_2NO_2$, and then reacted with NO to form N_2 and H_2O. Another possible reaction path is the adsorption of NH_3 on the surface of the catalyst and then the reaction with NO or nitrous acid. The intermediate produced NH_4NO_2 and NH_2NO decompose rapidly into N_2 and H_2O due to instability. Yu *et al.* found that NH_3 can be adsorbed on copper ion and the hydroxyl active position. NH_3 was first adsorbed on the Cu^{2+} site and then the NH_3 adsorbed on the B-acid position was re-migrated to the active position to participate in the NH_3-SCR reaction, and the B-acid position stored and supplied the NH_3 species to the active position [62].

The reaction mechanism must be understood to improve the performance of zeolite catalysts. The reaction mechanisms obtained on different zeolite catalysts vary, but they could be roughly divided into two categories, namely, the Eley-Rideal (E-R) mechanism and Langmuir-Hinshelwood (L-H) theory [48,49]. For E-R mechanism, the reactant NH_3 is initially adsorbed on the active site of the catalyst, and then react with NO_x in gas phase. By comparison, in L-H theory, NH_3 and NO_x are bound by the adjacent active sites adsorbed on the surface of the catalyst and decompose into N_2 and H_2O.

4. Performance of zeolite catalysts for NH_3-SCR

Zeolite catalysts such as SSZ-13 [63,64], ZSM-5 [65,66], SAPO-34 [67,68], and Beta [69,70] been received increasing attention for their NH_3-SCR reaction. Zeolites can be classified according to the number of atoms (T) in the ring, such as eight member ring (like LTA, GIS, CHA, AEI), ten member ring (like MFI), twelve member ring (like FAU, MOR, BEA) and ultra-large pore zeolite (the number of T in the pore is more than 12) [71]. Most zeolites have excellent adsorption properties, and suitable surface acidity and flexibility. By changing the type and existing state of active components on the surface or skeleton of zeolite, the active temperature of the catalyst could be changed accordingly. Furthermore, the active temperature could be controlled, and the anti-poisoning ability of the catalyst could be improved. The denitrification efficiency of the reported zeolites is shown in Table 1 [43,61,68,72–89].

4.1. Monometallic modified zeolite catalysts

Zeolites are modified with different metals, such as Cu, Fe, and Mn, for NH_3-SCR to obtain a high denitrification efficiency, high N_2 selectivity, and hydrothermal stability.

SSZ-13 has an excellent NH_3-SCR activity over a wide range of temperature, especially at low temperature. Cu-SSZ-13 was prepared from aluminosilicate gels by adding two structure-directing agents, namely, the *N*,*N*,*N*-trimethyl-1-adamantammonium and Cu-TEPA [90]. The results showed that the NO conversion could be maintained over 87% at low temperature (< 250 °C). Moreover, the decrease in catalytic activity under 250 °C was smaller than that at 250–475 °C due to the loss of some isolated Cu^{2+} ions and the surface acidity in the hydrothermally treated catalyst. Silicon carbide (SiC) as a support for SSZ-13 zeolite was investigated by Zhou *et al.* who found that the NO conversion increased with the Cu loading on Cu/SSZ-13@SiC within the range of 0.37–1.71 wt% [78]. The NO conversion over Cu(1.71)/SSZ-13@SiC was practically the same as that over Cu(4.03)/SSZ-13 below 250 °C. The use of the SiC support decreased the Cu loading compared with that of the unsupported Cu(4.03)/SSZ-13 and enhanced the catalytic activity of Cu/SSZ-13 in NH_3-SCR. In addition, Cu-LTA showed a wider temperature window and a better thermal stability than SSZ-13. Even after high hydrothermal aging, the $[Cu(OH)]^+$ species were remained over Cu-LTA. Jo *et al.* [53] investigated high-silica LTA zeolites and found that their NO conversion was similar at 200–250 °C (>40%). However, all copper-exchanged forms of LTA zeolites exhibited considerably higher activity maintenance than the current commercial Cu-SSZ-13 catalyst even after hydrothermal aging at 850 °C.

Cu-SSZ-39 (AEI structure) performs extremely well for the NH_3-SCR reaction with an extraordinary hydrothermal stability [75]. Comparing with Cu-SSZ-13, SSZ-39 zeolite contains more paired framework Al, leading to that Cu-SSZ-39 catalysts have more hydrothermally stable Cu^{2+}-2Z species, and this makes Cu-SSZ-39 accumulate less CuO_x during hydrothermal aging, and in consequence, the active Cu^{2+} species are more stable in the structure of Cu-SSZ-39 [76]. Martin *et al.* [77] found that the Cu-SSZ-39 catalysts prepared by one-pot and Cu ion-exchange methods were both showed excellent activity for SCR reaction.

Table 1
Temperature window and NO conversion of NH_3-SCR reaction.

Catalyst	SCR Temperature (°C)	NO conversion (%)	Ref.
Cu-SSZ-13	200–250	> 87	[72]
Mn-beta-Ac	150–250	50–97	[73]
Mn-ZSM-Ac		40–92	
Mn-beta-NO_3		40–90	
Mn-ZSM-NO_3		35–85	
Mn-ZMF-140	150–250	20–80	[74]
Cu-ZMF-140		5–85	
Cu-ZMF-25#3		20–98	
Cu–SSZ-39	170–250	43–98	[75]
Cu-SSZ-39	150–250	28–98	[76]
Cu-N-SSZ-39	175–250	32–93	[77]
Cu-SSZ-39"one pot"		28–98	
$Cu_{5.5}$-SAPO-44	150–250	10–90	[61]
$Cu_{3.3}$-SAPO-44-TEPA		85–99	
Cu-ZSM-5-(1∼6 h)	200–250	> 50	[78]
Cu-LTA(O)	200–250	20–93	[43]
Cu-LTA(E)AH		15–93	
Cu-LTA(E)AM		20–97	
Cu-LTA(E)PB		10–97	
Cu-SSZ-13		25–100	
Cu(4.03)-SSZ-13	150–250	33–98	[79]
Cu(0.37)-SSZ-13@SiC		< 10	
Cu(1.71)-SSZ-13@SiC		33–99	
2.60% Cu-ZSM-5	150–240	75–100	[80]
4.00% Cu-ZSM-5		45–100	
Hierarchical Fe-Beta	150–250	15–90	[81]
Fe-Beta		10–85	
Cu-SAPO-34	100–200	< 20	[68]
2.5 wt% Cu/BEA	150–250	25–99	[82]
2.6 wt% Cu-SAPO-34		45–93	
3.1 wt% Cu-SSZ-13		40–99	
Cu-M-5	200–250	90–99	[83]
Cu-M-6		93–98	
Cu(2.4)-M-5-A750		86–95	
Cu(4.0)-M-6-A750		92–96	
Cu(3.5)-9		85–95	
Cu(3.5)-9-A750		80–90	
Cu-SAPO-18-(1∼5)	175–250	35–100	[84]
Cu-Mn-ZSM-5	200–250	> 65	[85]
Cu-Mn-SAPO-34		> 90	
1.5 wt% Cu-CZC	150–250	75–87	[86]
7.4 wt% Fe-MOR		40–85	
(50%)Cu-CZC + (50%)Fe-MOR		60–92	
Cu-Fe-BEA	200–250	50–80	[87]
Cu-Fe-MOR		40–60	
Cu-Fe-FER		20–30	
Fe-ZSM-5	210–270	25–40	[88]
CS2		25–35	
CS2–2		55–85	
Ce-MS		15–20	
Ce-Cr	160–260	< 10	[89]
Mn-Ce/Ce-Zr	160–220	30–52	
Ce-Zr + H-Beta	160–260	60–85	
Mn-Ce/Ce-Zr + H-Beta	160–260	> 80	

SAPO-34 is also a small pore CHA. The NH_3-SCR activity of Cu-SAPO-34 could be influenced by the Si distribution to create different distributions and states of Cu species. Different Si distributions were generated by different templates. Chen *et al*. [82] prepared submicron Cu-SAPO-34 catalysts by using copper tetraethylenepentamine (Cu-TEPA) and morpholine (MOR) as templates [91]. The pure Cu-SAPO-34 catalysts had a higher NO conversion than Cu(3.5)-9 at 200−250 °C [92]. Even after 12 h of hydrothermal treatment, only a slight drop (< 5%) in the NO conversion over Cu(2.4)/M-5-A750 and Cu(4.1)/M-6-A750 was observed. However, the NO conversion over Cu(3.5)-9-A750 decreased by more than 5%, indicating that the submicron Cu-SAPO-34 catalysts synthesized with Cu-TEPA and MOR was more robust than Cu(3.5)-9 in the NH_3-SCR reaction. The reaction rate increased with copper loading up to 1.89 wt% under varying Cu contents (0.98–2.89 wt%) through the liquid ion exchange method [67]. SAPO-44 catalysts have a similar NH_3-SCR activity as SAPO-34. The NO conversion in Cu-SAPO-44 is lower than that in Cu-SAPO-44-TEPA (*via* a one-pot approach by combination of cyclohexylamine template and copper-amine complex) due to the strong coordinative effect of TEPA and the well-dispersed active Cu species [60]. More active Cu species would form after NH_4NO_3 treatment, which confirms the importance of TEPA for Cu dispersion in SAPO-44. SAPO-18 catalysts have a similar hydrothermal stability as SAPO-34 as a result of the presence of Si species in the CHA framework that leads to high hydrothermal stability. Different proportions of Si can affect the Si coordination structure of the catalysts, and then affect the acidity of Cu-SAPO-18 catalysts and the distribution of Cu, which in turn affect the activity of the catalyst. However, the Si content does not influence the NH_3-SCR reaction mechanism over Cu-SAPO-18 catalysts at 250 °C [83].

ZSM-5 catalysts with medium pores have a lower NO conversion than chabazite framework zeolites. Rutkowska *et al*. [74] investigated a micro-mesoporous catalyst with the properties of ZSM-5 zeolite *via* desilication with NaOH and NaOH/TPAOH (tetrapropylammonium hydroxide) and found that the NO conversion on the catalyst was more than 50% at 200−250 °C. Their results showed decreases in micropore volume and crystallinity of the samples and increases in surface acidity. Meanwhile, ZSM-5 zeolite generated mesoporosity. Moreover, the Cu^{2+} added to the micro-mesoporous samples was easily reduced to Cu^{+}. By increasing the Cu dispersion and stability of the bone, the ZSM-5 zeolites could be prepared *via* the hydrothermal synthesis of a copper complex precursor (EDTA-Cu) and a transparent solution in which the higher activity at 150−240 °C could maintain a high catalytic activity even after long-term heat and hydrothermal treatments [79]. To enhance the NO conversion of ZSM-5 catalysts and their potential for industrial applications, Gargiulo *et al*. [73] investigated ZSM-5 zeolite monolith foams (ZMFs) with a polyurethane foam (PUF) template. For Cu-ZMF-25#3, Mn-ZMF-140 and Cu-ZMF-140, the NO conversions were 20%–98%, 20%–80% and 5%–85%, respectively, within the temperature range of 150−250 °C. These structured catalysts exhibited the same specific catalytic activity as powdered counterparts, but they improved NO conversion due to the higher amount of catalyst per unit volume of the reactor and to their superior mass transfer coefficients coupled with low internal diffusion limitations.

Mn-based catalysts supported by ZSM and Beta have also attracted attention. Xu *et al*. used different Mn precursors to prepare Mn-ZSM-5 and Mn-Beta catalysts *via* wet impregnation. For Mn-beta-Ac, Mn-ZSM-Ac, Mn-beta-NO_3, and Mn-ZSM-NO_3 catalysts, the NO conversion at 150–250 °C were 50%–97%, 40%–92%, 40%–90% and 35%–85%, respectively. Mn-modified Beta zeolite has a suitable amount of weakly acidic centers, a high concentration of surface manganese, and a large presence of surface labile oxygen groups, properties that may be favorable for the catalytic performance at low temperatures [72].

Beta catalysts with large pores show lower NO conversion than small-pore chabazite catalysts. Leistner *et al*. [80] prepared three monolith catalysts and found that small-pore zeolites/silicoaluminophosphates with a CHA structure (Cu-SAPO-34 and Cu-SSZ-13) exhibited a higher SCR activity at 150−250 °C than Cu-BEA. However, the formation of ammonium nitrate species at 150 °C resulted in a gradual decrease in NO conversion, which was more stable on small-pore zeolites than on Cu-BEA. Furthermore, the results showed that the Cu in Cu-SAPO-34 was more easily reduced than that in Cu-SSZ-13, a process that could facilitate the redox processes. It was found that the pore structure could also affect the activities of Beta catalysts. Hierarchical zeolites contain both micro and meso-/macrospores, which can eliminate diffusion limitations and promote the accessibility of reactants to the active sites. Zhu *et al*. [81] investigated hierarchical Fe-Beta obtained by hydrothermal synthesis and found it exhibited higher low-temperature NH_3-SCR activity than that of the conventional Fe-Beta. Hierarchical Fe-Beta had more Lewis acid sites and isolated active Fe species, which may be associated with that the hierarchical structure introduced more structural defects as ion-exchange sites.

Various preparation methods result in diverse catalyst structures. Thus, varying denitrification performances are obtained. Furthermore, the type of metal species and the amount of metal loading also lead to different denitrification efficiencies due to the different chemical properties of catalyst surfaces. The SCR performance of monometallic modified zeolite catalysts depends on the amount of isolated ion sites, Si/Al ratios, and topological structures, which could affect the redox circle, acidic sites, and the channel structure [93].

4.2. Multi-metal modified zeolite catalysts

Adding other metals to enhance the performance of monometallic-modified zeolite catalysts have been considered. Thus, the synergistic catalysis of multi-metal-modified zeolite catalysts has been investigated. Li *et al*. prepared a series of bimetallic Fe-Mn/SBA-15 catalysts *via* the one-step incipient wetness impregnation method with the fly ash-derived SBA-15 as the porous support [85]. Their results showed that the NO conversion of Fe-Mn/SBA-15 (63%–90%) was higher than that of Mn/SBA-15 (20%–40%) and Fe/SBA-15 (< 45%) within the low-temperature range of 150−250 °C. Mn was added to improve the dispersion of Fe_2O_3 on the catalyst surface, whereas Fe was added to promote the formation of the single Beta-MnO_2 phase. SAPO-34 (CZC) and mordenite with transition metals Cu and Fe were studied by Hamoud *et al*. who found that 1.5 wt% Cu-CZC and 7.4 wt% Fe-MOR had SCR activities of 75%–87% and 40%–85%, respectively, at 150−250 °C [94]. In addition, (50%) Cu-CZC + (50%) Fe-MOR showed higher NH_3-SCR activity than Cu-CZC and Fe-MOR (above 85% at 200−250 °C) due to the synergistic effect between Cu and Fe metals and their good redox properties in the mixture. Jouini *et al*. exchanged a series of silica-rich zeolites with different pore structures (BEA, MOR, and FER) with Fe and Cu *via* the solid-state ion exchange method (SSIE) [86]. For Cu-Fe-BEA, Cu-Fe-MOR, and Cu-Fe-FER, the NO conversions were 50%–80%, 40%–60% and 20%–30%, respectively, at 200−250 °C, indicating that the zeolite framework was one of the parameters controlling the amount, environment, and distribution of the metal species formed during the ion exchange process in Cu-Fe-zeolite catalysts. Wang *et al*. [88] prepared CuFe-SSZ-13 catalysts by using three different methods including solid-state ion-exchange (SSIE), homogeneous deposition precipitation (HDP) and liquid ion-exchange (IE). Given the high Cu loading and more isolated Cu^{2+}, CuFe-SSZ-13_{SSIE} showed the highest NH_3-SCR activity at 150−250 °C than the others. Meanwhile, the

hydrothermal stability of the three CuFe-SSZ-13 catalysts was also significantly different. The results indicated that different methods affect the composition of active species, ultimately leading to different NH_3-SCR activities. Cu-Mn bimetal catalysts was prepared using a two-step liquid ion exchange method by Zhao *et al.* [84]. The NO conversion on Cu-Mn/ZSM-5 exceeded 65% at 200–250 °C, whereas that on Cu-Mn/SAPO-34 surpassed 90%. The results showed that the activity of Cu-Mn/SAPO-34 was more stable than that of Cu-Mn/ZSM-5, showing a higher NO conversion below 200 °C due to the larger BET surface area and the greater pore volume. Ce could reportedly inhibit the deposition of NH_4HSO_4 on the surface of catalysts and prefers to react with SO_2 to protect active metal sites. Zhang *et al.* [87] prepared a core-shell structured Fe-ZSM-5@Ce/mesoporous silica and reported that all Fe species were in the Fe-ZSM-5 core while the Ce species mostly remained within the channels of the mesoporous silica shell. The mesoporous silica shell highly promoted the dispersion of CeO_2 with its confinement effect, resulting in a strong redox ability due to the enhancement of the interaction between active species and supports. Enough space was also provided for the oxidation of NO. Thus, the CS2–2 sample showed stronger NO absorbability and oxidizability. Stakheev *et al.* [95] investigated the combined catalysts by the mechanical mixing of the redox (CeO_2-ZrO_2 or Mn-Ce/CeO_2-ZrO_2) and zeolite components (Fe-Beta, H-Beta, USY). For [Ce-Zr + H-Beta] and [Mn-Ce/Ce-Zr + H-Beta], the NO conversion was 60%–80% and more than 85%, respectively, at 160–260 °C, indicating that significant enhancement of $DeNO_x$ activity compared with the individual component activities.

The interaction between active species and supports could be enhanced, and the dispersion of the active metal could be promoted by modifying zeolite catalysts with multi-metals. The synergistic effect between metals and supports facilitate the redox properties of multi-metal-modified zeolite catalysts, which could facilitate the denitrification process.

5. Sulfur and water poisoning on NH_3-SCR reaction over zeolite catalysts

In practical application conditions, both the stationary sources flue gas and vehicle exhaust contain a certain amount of H_2O and SO_2. H_2O and SO_2 have toxic effects on catalysts [96,97]. When water exists in the form of water vapor, the toxicity of alkali metal soluble salt such as Na and K to catalysts is aggravate. The competitive physical adsorption of water vapor with NO and NH_3 on the surface of catalysts would expand and damage the structure of the catalysts, consequently rupturing the catalyst and decreasing the denitrification activity [98]. The SO_2 would be oxidized to SO_3, which would react with NH_3 and produce $(NH_4)_2SO_4$ and/or NH_4HSO_4, which in turn would block and destroy the active sites. Furthermore, the SO_2 could lead to the sulfation of active components and result to the deactivation of the catalyst. Therefore, many researchers have explored the effect of H_2O and SO_2 on catalysts. The results are shown in Table 2 [94,95,99–102].

Dahlin *et al.* reported the important impact of SO_2-exposure temperature on the deactivation of Cu-SSZ-13 catalysts [102]. The deactivation at the sulfur-exposure temperature of 220 °C was worse than that at 280 °C. Part of the sulfur-exposed samples showed that this trend was caused by the absorption of more sulfur on the catalyst at the lower sulfur-exposure temperatures. In addition, the effect of SO_2 on the standard SCR reaction was greater than that of the fast SCR reaction. Luo *et al.* prepared commercial Cu-SSZ-13 catalysts to reveal their unique responses to sulfur poisoning [100]. The NO conversion in fresh Cu-SSZ-13 catalysts exceeded 90% at 200–250 °C and within 60%–80% after sulfur exposure. Obviously, sulfur poisoning affected the low-temperature NO conversion in NH_3-SCR activity. The decreased interaction of Cu ions with the zeolite framework upon sulfur exposure suggested that Cu ions interacted strongly with sulfur.

Table 2
Sulfur and water resistance of zeolites in NH_3-SCR reaction.

Catalyst	SCR temperature (°C)	WR* (%)	SR** (%)	Ref.
Fe-Mn-SBA-15	150–250	10 (200 °C)	–	[94]
Mn-SBA-15	150–250			
Fe-SBA-15	150–250			
Fe-Mn-SBA-15	200			
Fe-Mn-SBA-15(H_2O)	200			
Cu-SSZ-13$_{SSIE}$	150–250	22–47	5–30	[95]
Cu-SSZ-13$_{HDP}$				
Cu-SSZ-13$_{IE}$				
Cu-SSZ-13(S)				
Cu-SSZ-13(S+H)				
CuFe-SSZ-13				
CuFe-SSZ-13(S)				
CuFe-SSZ-13(S+H)				
Cu-SSZ-39	150–250	–	10–43	[99]
S-200				
S-200-R				
Cu-SAPO-34	150–250	–	12–40	[100]
Cu-SAPO-34(SO_2-1A)				
Cu-SAPO-34(SO_2-1E)				
Cu-SAPO-34(SO_2-2A)				
Cu-SAPO-34(SO_2-2E)				
Cu-SSZ-13	200–250	–	60–80	[101]
Cu-SSZ-13(SO_2)				
Cu-SSZ-13	180–250	–	73–78	[102]
SO_x				
Regen 550 °C				
Regen 650 °C				
Regen 700 °C				

WR*: Water resistance (the decreased rate of NO conversion).
SR**: SO_2 resistance (the decreased rate of NO conversion).

The introduction of other metal species, such as Fe and Ce, could protect the active center and achieve the purpose of resisting sulfur to improve the low-temperature NH_3-SCR activity. Wang *et al.* prepared three CuFe-SSZ-13 catalysts that showed similar SO_2 and water resistances and were better than that of Cu-SSZ-13 [88]. The results indicated that the improvement was caused by the Fe loading, especially at low temperature. Fe preferred to react with SO_2 to protect the Cu active site. Ce is known to combine easily with SO_2. During the NH_3-SCR reaction, SO_2 first combined with Ce rather than the active metal [87,95]. Du *et al.* [99] investigated the effects of sulfation on Cu-SSZ-39 catalyst at 200 °C, and found that the coverage of active sites by H_2SO_4 and the formation of stable $CuSO_4$ species was the reason for the deactivation. After regeneration at 600 °C, H_2SO_4 decomposed for the S-200, so the catalytic activity partly recovered.

Wijayanti *et al.* [89] found that the storage and release of ammonia on the sulfur-poisoned sample were only slightly lower than those on the fresh catalyst. In addition, sulfur bonded strongly to the catalyst sites indicating the availability of few copper in the poisoned sample that could undergo a redox cycle. A second sulfur poisoning was conducted on the same monolith and produced a similar trend, that is, high initial deactivation was followed by the gradual increase in activity after repeated SCR experiments. Hammershøi *et al.* [101] found that the NO conversion at 200–250 °C was lower than for the fresh catalysts in all measurements at both sulfated and regenerated states. Their results showed that the S/Cu ratios were always lower than 1, indicating that the uptake of sulfur was related to the adsorption of SO_2 on Cu. In addition, ammonium sulfate did not precipitate in the catalysts when co-feeding SO_2, H_2O and NH_3 due to the SO_2 related to the Cu sites.

Mn-Fe zeolite catalysts show excellent low temperature NH_3-SCR activity and water-resistance. Li *et al.* examined the long-term

stability of Fe-Mn/SBA-15 in the presence of water [85]. Their results showed that the catalyst had significant recovery characteristics after stopping the feed of H_2O, indicating that H_2O did not result in the permanent deactivation of catalysts. The NO conversion on the Fe-Mn/SBA-15 catalyst dropped by 10% only during the entire 200 h durability test. Constructing a specific core-shell structure [103] could establish a hydrophobic protective layer in zeolite catalysts to inhibit H_2O adsorption and improve the SCR reaction.

Recent studies demonstrated that H_2O mainly reduces the conversion of NO_x by the competitive adsorption with NO and NH_3. The effect of H_2O on competitive adsorption decreases with the increase in temperature. Furthermore, the existence of H_2O affects the oxidation of catalysts and the rate of catalytic reaction. However, the effect of H_2O on catalysts is mostly reversible. The effect of SO_2 on catalysts is the competitive adsorption between SO_2 and NO and NH_3 reactants [104]. SO_2 first combines with doped metal rather than active metal in the NH_3-SCR reaction to protect the active center. Meanwhile, the formation of ammonium sulfate from SO_2 and NH_3 clogs the surface of the catalysts. If the reaction temperature is higher than the decomposition temperature of ammonium sulfate (ammonium sulfate, 280 °C; ammonium hydrogen sulfate, 350 °C), the ammonium sulfate would not deposit. Ammonium sulfate is soluble in water. Therefore, the effect can often be regenerated and restored by water washing and pyrolysis [105]. In addition, the formation of sulfate from SO_2 and metal active components directly leads to the deactivation of active components of catalysts [106]. The decomposition temperature of metal sulfate was usually much higher than that of low temperature NH_3-SCR. Therefore, this effect would lead to the irreversible inactivation of the catalysts in the entire low-temperature range.

The hydrophobicity of catalysts can be increased to improve the resistance of catalysts to H_2O. The adsorption and oxidation of NO could also be improved by increasing the oxygen vacancy on the surface of catalysts. This step could alleviate the competitive adsorption of nitrate by H_2O [107,108]. As for improving the resistance of catalysts to SO_2, the ability to inhibit the conversion of SO_2 to sulfate by doping other elements could be used to alleviate the degree of sulfation of metal elements. The deposition of ammonium sulfate could also be weakened by support loading and the construction of a special structure [109,110].

6. Conclusion and prospects

NH_3-SCR reaction is one of the most popular technologies, and zeolite catalysts have received increasing attention due to their wide active temperature window, high catalytic activity, good thermal stability and low SO_2 oxidation ability. The type and strength of interaction between the zeolite support and the active component affect the catalytic activity and the sulfur and water poisoning performance of catalysts. We reviewed the mechanism of NH_3-SCR reaction on zeolites and the comparison of the denitrification performance of zeolite catalysts prepared by different methods. The effects of sulfur and water poisoning on NH_3-SCR reaction on zeolite catalysts were also analyzed. Small pore chabazite framework zeolites were found to have better NO reduction characteristics for a wide temperature window than large and medium pore zeolites. Furthermore, the methods for improving the resistance of zeolite catalysts to sulfur and water were conducted, such as doping other elements and improving the hydrophobicity of catalysts. Nevertheless, several challenges must be overcome to expand the use of zeolite catalysts in NH_3-SCR reaction.

The preparation of existing zeolite catalysts requires various raw materials and involves several preparation steps. Therefore, researchers must develop zeolite catalysts with low raw material costs and simple preparation methods. Besides, according to a recent study, several preliminary mechanisms for the sulfur and water poisoning of low-temperature zeolite catalysts exist. However, the dynamic process and microscopic reaction mechanisms of sulfur and water poisoning have not been thoroughly studied and hence require further studies. Furthermore, experiments and theoretical calculation must be combined to study the NH_3-SCR reaction on zeolites catalysts at low temperature and deepen the understanding of the mechanism for the deNO_x process and the sulfur and water resistance of zeolite catalysts, and zeolite catalysts with long-term tolerance to water and sulfur poisoning in low-temperature conditions must be developed to satisfy the requirements of industrial applications. Especially for the sulfur and water resistance of zeolite catalysts there still remain some probably strategies to do, such as reducing the adsorption/oxidation of SO_2, improving the adsorption of active intermediate species in the coexistence of sulfate species and sulfuric acid, replacing with other ion to protect active sites, facilitating the decomposition of sulfate and constructing a specific core−shell structure to establish a protective layer.

Declaration of competing interest

The authors declare that they have no known competing financial interests or personal relationships that could have appeared to influence the work reported in this paper.

Acknowledgment

This work was supported by the Sichuan Science and Technology Program (No. 2019YFS0495-02).

References

[1] M. Al-Harbi, A. Al-majed, A. Abahussain, Environ. Eng. Res. 25 (2020) 147–162.
[2] L. Wang, J. Wang, X. Tan, C. Fang, Atmosphere 11 (2020) 30.
[3] M. Radojevic, Reduction of nitrogen oxides in flue gases, in: K.W. van der Hoek, W. Klaas (Eds.), Nitrogen, the Confer-N-s, Elsevier, Amsterdam, 1998, pp. 685–689.
[4] F. Nakajima, I. Hamada, Catal. Today 29 (1996) 109–115.
[5] F. Luck, J. Roiron, Catal. Today 4 (1989) 205–218.
[6] P. Ciambelli, L. Lisi, G. Russo, J.C. Volta, Appl. Catal. B 7 (1995) 1–18.
[7] A. Fritz, V. Pitchon, Appl. Catal. B 13 (1997) 1–25.
[8] X. Cheng, X.T. Bi, Particuology 16 (2014) 1–18.
[9] K. Skalska, J.S. Miller, S. Ledakowicz, Sci. Total Environ. 408 (2010) 3976–3989.
[10] R.M. Heck, Catal. Today 53 (1999) 519–523.
[11] M. Shelef, Chem. Rev. 95 (1995) 209–225.
[12] S. Yu, Y. Lu, F. Gao, L. Dong, Catal. Today 339 (2020) 265–273.
[13] Q. Zhang, Y. Zhang, T. Zhang, et al., Appl. Surf. Sci. 503 (2020) 144190.
[14] G. Chi, B. Shen, R. Yu, C. He, X. Zhang, J. Hazard. Mater. 330 (2017) 83–92.
[15] J. Li, M. Hu, S. Zuo, X. Wang, Curr. Opin. Chem. Eng. 20 (2018) 93–98.
[16] H. Zhao, X. Luo, H. Zhang, et al., Greenhouse Gases: Sci. Technol. 8 (2018) 11–36.
[17] P. Wang, L. Yao, Y. Pu, et al., RSC Adv. 9 (2019) 36658–36663.
[18] T. Selleri, F. Gramigni, I. Nova, E. Tronconi, Appl. Catal. B 225 (2018) 324–331.
[19] M. Pourkhalil, N. Izadi, A. Rashidi, M. Mohammad-Taheri, Mater. Res. Bull. 97 (2018) 1–5.
[20] L. Xu, C. Wang, H. Chang, et al., Environ. Sci. Technol. 52 (2018) 7064–7071.
[21] M. Kobayashi, M. Hagi, Appl. Catal. B 63 (2006) 104–113.
[22] M. Fu, C. Li, P. Lu, et al., Catal. Sci. Technol. 4 (2014) 14–25.
[23] H. Jiang, B. Guan, X. Peng, et al., Chem. Eng. J. 379 (2020) 122358.
[24] Z. Wu, B. Jiang, Y. Liu, H. Wang, R. Jin, Environ. Sci. Technol. 41 (2007) 5812–5817.
[25] A. Sultana, M. Haneda, T. Fujitani, H. Hamada, Microporous Mesoporous Mater. 111 (2008) 488–492.
[26] Y.H. Chin, W.E. Alvarez, D.E. Resasco, Catal. Today 62 (2000) 159–165.
[27] C. Gao, J.W. Shi, Z. Fan, G. Gao, C. Niu, Catalysts 8 (2018) 11.
[28] J.K. Lai, I.E. Wachs, ACS Catal 8 (2018) 6537–6551.
[29] I. Salem, X. Courtois, E. Corbos, P. Marecot, D. Duprez, Catal. Commun. 9 (2008) 664–669.
[30] R. You, M. Meng, J. Zhang, et al., Catal. Today 327 (2019) 347–356.
[31] Z. Liu, S. Zhang, J. Li, L. Ma, Appl. Catal. B 144 (2014) 90–95.
[32] D. Fang, F. He, X. Liu, et al., Appl. Surf. Sci. 427 (2018) 45–55.

[33] F. Gao, X. Tang, H. Yi, et al., Appl. Surf. Sci. 443 (2018) 103–113.
[34] K. Zhao, J. Meng, J. Lu, et al., Appl. Surf. Sci. 445 (2018) 454–461.
[35] N.R. Jaegers, J.K. Lai, Y. He, et al., Angew. Chem. Int. Ed. 58 (2019) 12609–12616.
[36] C. Chen, Y. Cao, S. Liu, J. Chen, W. Jia, Chin. J. Catal. 39 (2018) 1347–1365.
[37] M. Qing, S. Su, L. Wang, et al., Chem. Eng. J. 361 (2019) 1215–1224.
[38] R. Ning, L. Chen, E. Li, X. Liu, T. Zhu, Catalysts 9 (2019) 220.
[39] Y. Xu, X. Wu, Q. Lin, et al., Appl. Catal. A 570 (2019) 42–50.
[40] T. Ye, D. Chen, X. Zeng, IOP Conf. Ser.: Earth Environ. Sci. 108 (2018) 052055.
[41] S. Youn, I. Song, H. Lee, S.J. Cho, D.H. Kim, Catal. Today 303 (2018) 19–24.
[42] D. Chen, C. Cen, J. Feng, et al., J. Chem. Technol. Biotechnol. 91 (2016) 2842–2851.
[43] Z. Han, Q. Yu, H. Xie, et al., Environ. Sci. Pollut. Res. 25 (2018) 32122–32129.
[44] H. Xu, N. Yan, Z. Qu, et al., Environ. Sci. Technol. 51 (2017) 8879–8892.
[45] B. Samojeden, T. Grzybek, Energy 116 (2016) 1484–1491.
[46] M. Wang, H. Liu, Z. Huang, F. Kang, Chem. Eng. J. 256 (2014) 101–106.
[47] J. Han, D. Zhang, P. Maitarad, et al., Catal. Sci. Technol. 5 (2015) 438–446.
[48] H. Wang, X. Li, F. Meng, G. Wang, D. Zhang, Chem. Eng. J. 392 (2019) 123798.
[49] W. Li, R. Guo, S. Wang, et al., Fuel Process. Technol. 154 (2016) 235–242.
[50] S. Wang, R. Guo, W. Pan, et al., Catal. Commun. 89 (2017) 143–147.
[51] A. Wang, Y. Wang, E.D. Walter, et al., Catal. Today 320 (2019) 91–99.
[52] T. Selleri, I. Nova, E. Tronconi, V. Schmeisser, S. Seher, Catal. Today 320 (2019) 100–111.
[53] D. Jo, G.T. Park, T. Ryu, S.B. Hong, Appl. Catal. B 243 (2019) 212–219.
[54] G. Busca, L. Lietti, G. Ramis, F. Berti, Appl. Catal. B 18 (1998) 1–36.
[55] H. Hamada, Catal. Today 22 (1994) 21–40.
[56] C. Resini, T. Montanari, L. Nappi, et al., J. Catal. 214 (2003) 179–190.
[57] S. Suárez, J. Martín, M. Yates, P. Avila, J. Blanco, J. Catal. 229 (2005) 227–236.
[58] C. Ciardelli, I. Nova, E. Tronconi, et al., Appl. Catal. B 70 (2007) 80–90.
[59] X.F. Tang, J.H. Li, L.A. Sun, J.M. Hao, Appl. Catal. B 99 (2010) 156–162.
[60] Y. Xin, N. Zhang, X. Wang, et al., Catal. Today 332 (2019) 35–41.
[61] G. Zhou, B. Zhong, W. Wang, et al., Catal. Today 175 (2011) 157–163.
[62] T. Yu, H. Teng, D. Fan, J. Wang, L. Wei, J. Phys. Chem. C 118 (2014) 6565–6575.
[63] Y. Cui, Y. Wang, D. Mei, et al., J. Catal. 378 (2019) 363–375.
[64] J.H. Kwak, R.G. Tonkyn, D.H. Kim, J. Szanyi, C.H.F. Peden, J. Catal. 275 (2010) 187–190.
[65] X. Lou, P. Liu, J. Li, Z. Li, K. He, Appl. Surf. Sci. 307 (2014) 382–387.
[66] F. Bin, C. Song, G. Lv, et al., Appl. Catal. B 150 (2014) 532–543.
[67] J. Xue, X. Wang, G. Qi, et al., J. Catal. 297 (2013) 56–64.
[68] L. Wang, W. Li, G. Qi, D. Weng, J. Catal. 289 (2012) 21–29.
[69] Y. Zhu, B. Chen, R. Zhao, et al., Catal. Sci. Technol. 6 (2016) 6581–6592.
[70] A. Corma, V. Forne, E. Palomares, Appl. Catal. B 11 (1997) 233–242.
[71] C. Baerlocher, W. Meier, D.H. Olson, Atlas of Zeolite Framework Types, 5th ed., Elsevier, Amsterdam, 2001.
[72] W. Xu, G. Zhang, H. Chen, et al., Chin. J. Catal. 39 (2018) 118–127.
[73] N. Gargiulo, D. Caputo, G. Totarella, L. Lisi, S. Cimino, Catal. Today 304 (2018) 112–118.
[74] M. Rutkowska, I. Pacia, S. Basąg, et al., Microporous Mesoporous Mater. 246 (2017) 193–206.
[75] M. Moliner, C. Franch, E. Palomares, M. Grill, A. Corma, Chem. Commun. 48 (2012) 8264–8266.
[76] Y. Shan, W. Shan, X. Shi, et al., Appl. Catal. B 264 (2020) 118511.
[77] N. Martín, C.R. Boruntea, M. Moliner, A. Corma, Chem. Commun. 51 (2015) 11030–11033.
[78] T. Zhou, Q. Yuan, X. Pan, X. Bao, Chin. J. Catal. 39 (2018) 71–78.
[79] E. Yuan, K. Zhang, G. Lu, Z. Mo, Z. Tang, J. Ind, Eng. Chem. 42 (2016) 142–148.
[80] K. Leistner, O. Mihai, K. Wijayanti, et al., Catal. Today 258 (2015) 49–55.
[81] N. Zhu, Z. Lian, Y. Zhang, W. Shan, H. He, Chin. Chem. Lett. 30 (2019) 867–870.
[82] Z. Chen, C. Fan, L. Pang, et al., Appl. Surf. Sci. 448 (2018) 671–680.
[83] Z. Chen, C. Fan, L. Pang, et al., Chem. Eng. J. 348 (2018) 608–617.
[84] S. Zhao, L. Huang, B. Jiang, M. Cheng, J. Zhang, Y. Hu, Chin. J. Catal. 39 (2018) 800–809.
[85] G. Li, B. Wang, H. Wang, et al., Catal. Commun. 108 (2018) 82–87.
[86] H. Jouini, I. Mejri, J. Martinez-Ortigosa, et al., Solid State Sci. 84 (2018) 75–85.
[87] L. Zhang, T. Du, H. Qu, B. Chi, Q. Zhong, Chem. Eng. J. 313 (2017) 702–710.
[88] Y. Wang, L. Xie, F. Liu, W. Ruan, J. Environ. Sci. 81 (2019) 195–204.
[89] K. Wijayanti, S. Andonova, A. Kumar, et al., Appl. Catal. B 166 (2015) 568–579.
[90] C. Fan, Z. Chen, L. Pang, et al., Chem. Eng. J. 334 (2018) 344–354.
[91] R. Martínez-Franco, M. Moliner, C. Franch, A. Kustov, A. Corma, Appl. Catal. B 127 (2012) 273–280.
[92] R. Martínez-Franco, M. Moliner, P. Concepcion, J.R. Thogersen, A. Corma, J. Catal. 314 (2014) 73–82.
[93] L. Han, S. Cai, M. Gao, et al., Chem. Rev. 119 (2019) 10916–10976.
[94] H.I. Hamoud, V. Valtchev, M. Daturi, Appl. Catal. B 250 (2019) 419–428.
[95] A.Y. Stakheev, A. Mytareva, D. Bokarev, et al., Catal. Today 258 (2015) 183–189.
[96] G. Liu, W. Zhang, P. He, et al., Catalysts 9 (2019) 289.
[97] H. Wang, B. Huang, C. Yu, et al., Appl. Catal. A 588 (2019)117207.
[98] G. Centi, F. Vazzana, Catal. Today 53 (1999) 683–693.
[99] J. Du, X. Shi, Y. Shan, G. Xu, Y. Sun, Catal. Sci. Technol. 10 (2020) 1256–1263.
[100] J. Luo, D. Wang, A. Kumar, et al., Catal. Today 267 (2016) 3–9.
[101] P.S. Hammershøi, P.N. Vennestrøm, H. Falsig, A.D. Jensen, T.V. Janssens, Appl. Catal. B 236 (2018) 377–383.
[102] S. Dahlin, C. Lantto, J. Englund, et al., Catal. Today 320 (2019) 72–83.
[103] T. Du, H. Qu, Q. Liu, Q. Zhong, W. Ma, Chem. Eng. J. 262 (2015) 1199–1207.
[104] L. Huang, X. Wang, S. Yao, et al., Catal. Commun. 81 (2016) 54–57.
[105] C. Yu, B. Huang, L. Dong, et al., Chem. Eng. J. 316 (2017) 1059–1068.
[106] C. Yu, B. Huang, L. Dong, C. Feng, X. Liu, Catal. Today 281 (2016) 610–620.
[107] F. Gao, D. Mei, Y. Wang, Jn. Szanyi, C.H. Peden, J. Am. Chem. Soc. 139 (2017) 4935–4942.
[108] K. Zha, L. Kang, C. Feng, et al., Environ. Sci.: Nano 5 (2018) 1408–1419.
[109] Z. Wang, Q. Sun, D. Wang, et al., Sep. Purif. Technol. 209 (2019) 1016–1026.
[110] X. Li, J. Feng, Z. Xu, et al., React. Kinet. Mech. Catal. 128 (2019) 163–174.